Supplementary Materials:

Supplemental Methods

Cells and cell lines

Human umbilical vein endothelial cells (HUVECs) were purchased and maintained using EGM™ BulletKit™ (Lonza, Walkersville, MD). *Drosophila* S2 cells were maintained in Schneider's complete medium and transitioned to serum free Insect-Xpress (Lonza, Walkersville, MD) supplemented with 0.5 mM $CuSO_4$ for recombinant protein expression. Anti-human ICAM-1 hybridoma (clone R6.5), CHO-hICAM, and CHO-K1 wild type cells were purchased from ATCC (Manassas, VA).

Antibodies and other reagents

Human α-thrombin, human PC, corn trypsin inhibitor (CTI), and blood collection tubes containing citrate and CTI were purchased from Haematologic Technologies (Essex Junction, VT). Recombinant human TNF-α was purchased from Corning (Corning, NY). Lipopolysaccharides (LPS) from *E. Coli* 055:B5 and recombinant hirudin were purchased from Sigma-Aldrich (St Louis, MO). Anti-human VCAM-1 (polyclonal, BBA19) was purchased from R&D systems (Minneapolis, MN). Anti-human TF antibodies were purchased from R&D systems (Minneapolis, MN) and eBioscience (clone HTF-1, San Diego, CA). FITC conjugated-anti-CD41 (clone HIP8) was also purchased from eBioscience. Anti-human TM (clone Phx-01) and Brilliant Violet anti-CD45 (clone 30-F11) antibodies were purchased from BioLegend (San Diego, CA). Lyophilized, immunodepleted PC-deficient plasma and normal plasma controls were purchased from Aniara (West Chester, OH).

Cloning of R6.5 single chain variable fragment (scFv), soluble human TM (*shTM), and the hTM/R6.5 fusion protein*

PCR using 5' signal peptide primers was used to isolate full length cDNAs for R6.5 variable heavy chain (V_H) and light chain (V_L) from hybridoma-derived single stranded cDNA, as previously described[33]. The encoded sequence was compared with the previously published full-length sequence of the R6.5 monoclonal antibody (mAb) variable domains and found to be identical[34]. V_H and V_L cDNAs were assembled into an scFv construct in the pMT/Bip expression vector with the triple flag tag appended to the 3' end of the V_L domain.

Likewise, cDNAs encoding shTM (Glu22-Ser515) and the hTM/R6.5 fusion protein were ligated into the pMT/Bip expression vector (Invitrogen, Carlsbad, CA), each with a triple Flag tag appended to the 3' end. For the fusion protein, an Spe I site was added to the 5' end of R6.5 scFv and the 3' end of shTM, along with a 13 amino acid rigid linker ($(SSSSG)_2AAA$).

Recombinant protein expression and purification

pMT/shTM, R6.5 scFv, and hTM/R6.5 were each co-transfected with pCoBLAST in S2 cells and selected with blasticidin to generate stable cell lines[23]. Expression and purification was performed as previously described[23]. Briefly, proteins were harvested from S2 cell supernatant using an anti-FLAG (M2) affinity column (Sigma Aldrich), and assessed for purity via SDS-PAGE and HPLC.

Figures S1-S8

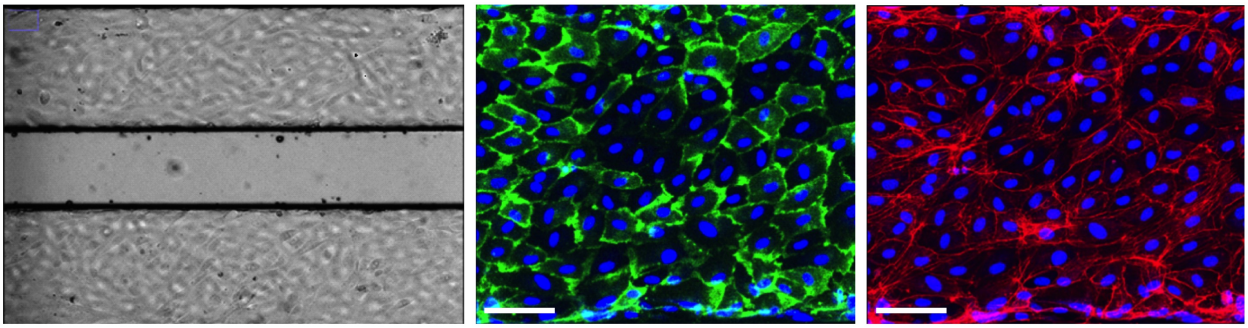

Figure. S1. Confocal microscopy of an endothelialized microvessel. Endothelialized channel was fixed and stained for CD31/PECAM-1 (green) and actin (red), and with DAPI (blue). Projected z-stacks show the monolayer on the bottom surface of the channel, demonstrating a typical pattern of expression of PECAM-1, localized predominantly at endothelial cell-cell junctions.

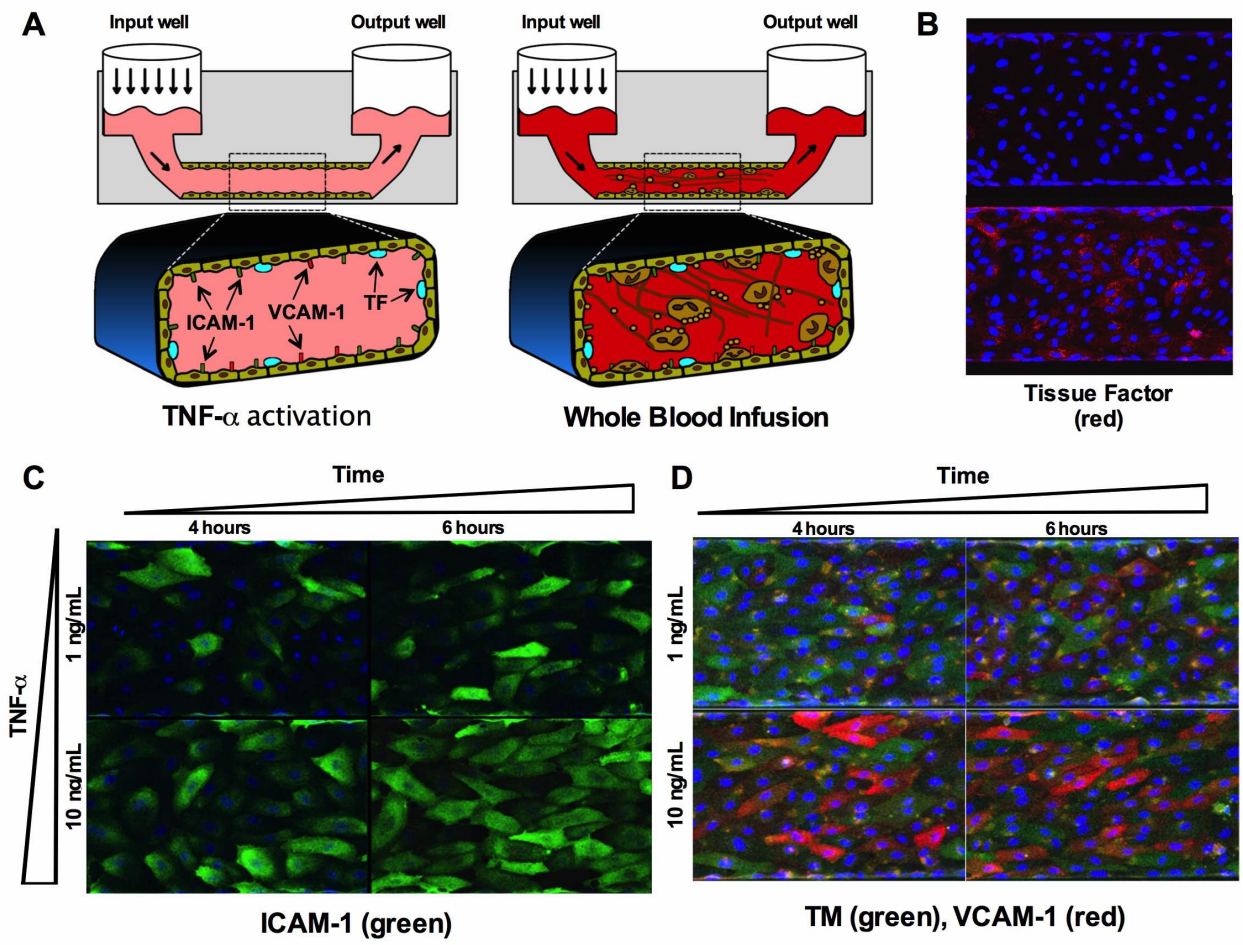

Figure S2. Microfluidic model of inflammatory microvascular thrombosis. (A) Schematic illustrating experimental protocol: endothelialized channels are activated with TNF-α during 6 hour flow adaptation, followed by 30 min TNF-α washout period and infusion of WB. (B) Confocal microscopy demonstrates TNF-α dependent expression of TF (top panel - untreated, bottom panel – 10ng/mL for 6 hours). Activated endothelial monolayers show dose (1 and 10 ng/mL shown) and time (4 and 6 hours) dependent expression of (C) ICAM-1 and (D) VCAM-1 and suppression of TM.

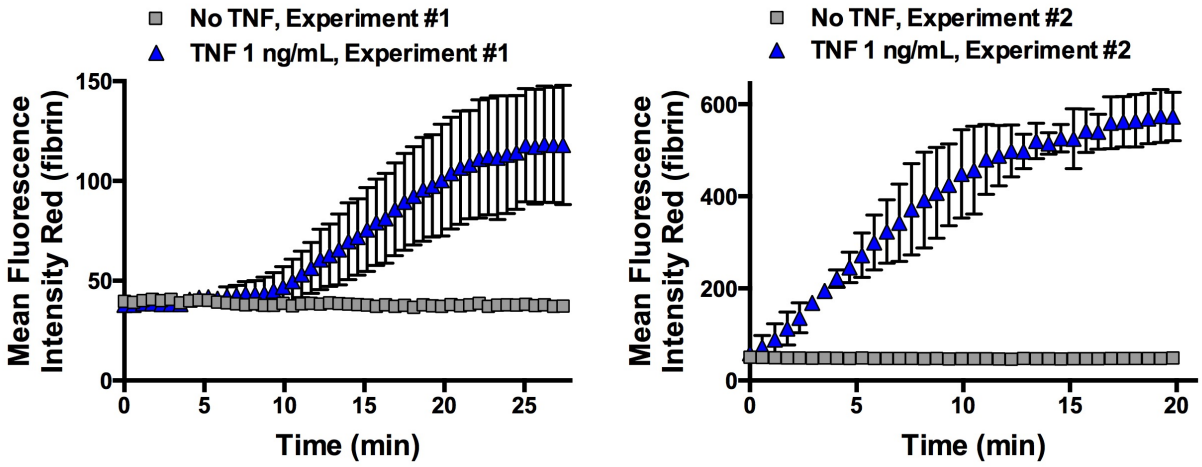

Figure S3. Intra- vs. Inter-experimental variability. Fibrin deposition data from two independent experiments. While some variation is seen between replicate channels within the same experiment (error bars show mean ± SEM for n = 2-3 channels), the timing and extent of fibrin deposition is fairly consistent, allowing meaningful statistical comparisons between experimental groups. In contrast, the MFI vs. time curve is markedly different between TNF-α stimulated channels run on separate days, preventing pooling of data or comparisons of groups run on separate days.

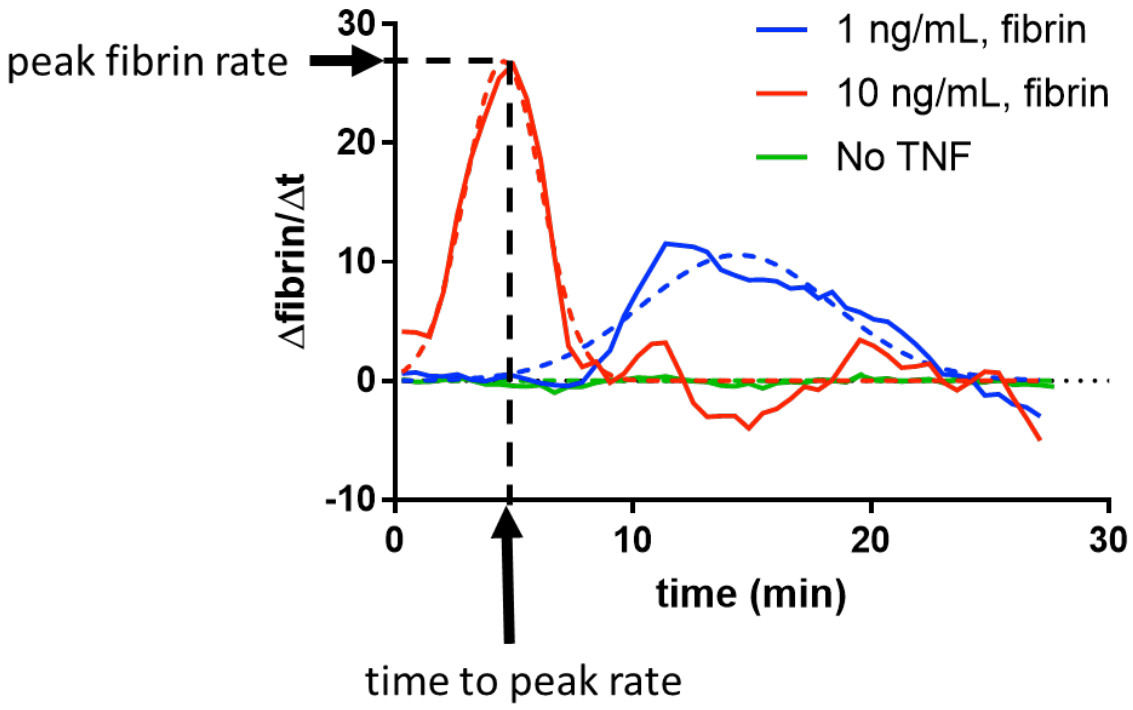

Figure S4. Additional analysis of the data shown in Figure 2, generated by graphing the first derivative of fibrin fluorescence intensity (dF/dt) over time. Raw data (solid lines) are analogous to thrombin generation (TG) curves generated in standard thrombin generation assays and can be fitted to Gaussian curves (dotted lines) to enable derivation of various parameters, including time to peak fibrin generation and peak fibrin generation rate (see Table S1).

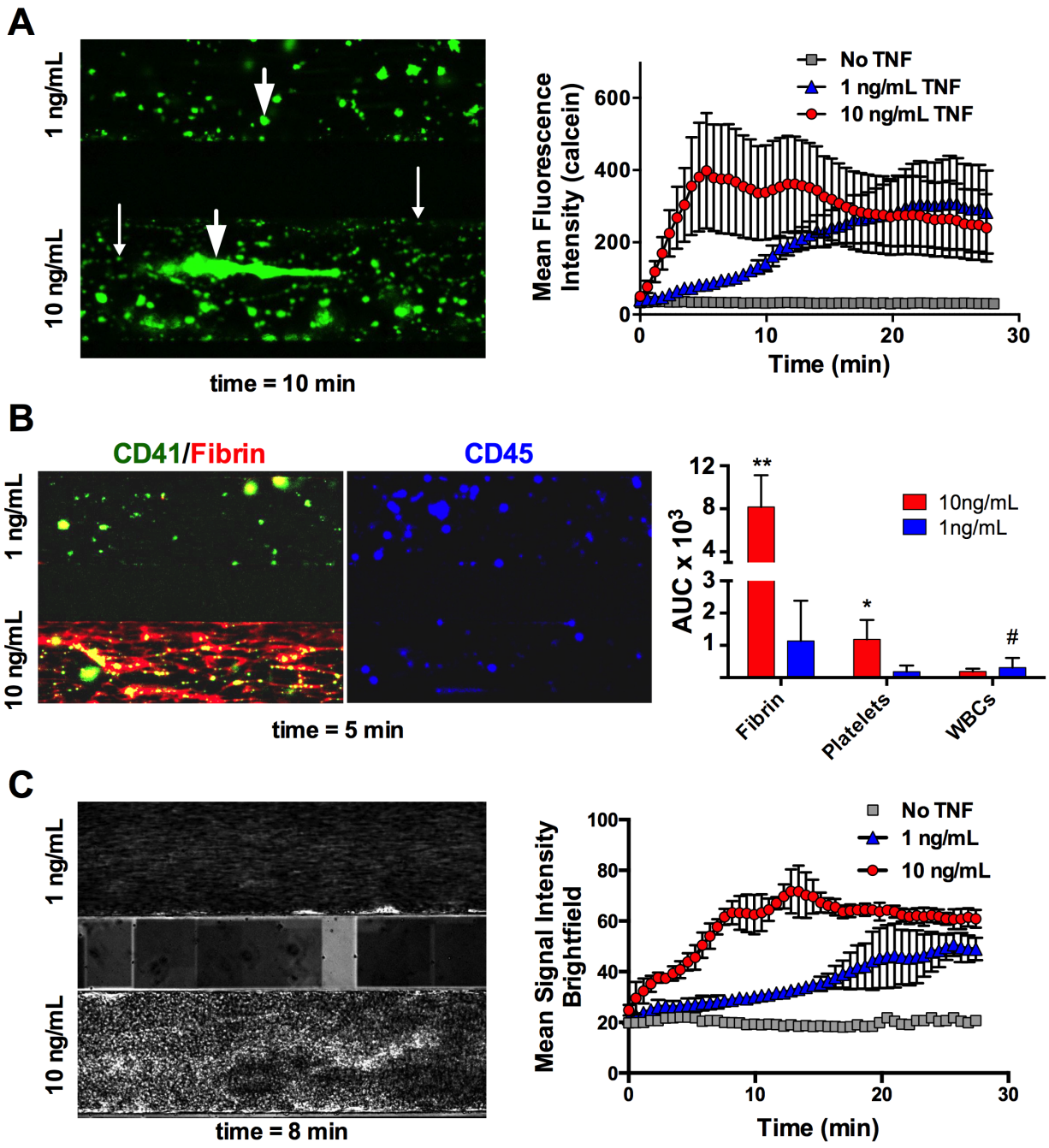

Figure S5. (A) Green fluorescence, representing adhesion of leukocytes and platelets (both labeled with calcein AM) to the endothelium. Representative image (left panel) shows individual adherent leukocytes (arrows) as well as variably sized clusters of various cell types (arrowheads). Graph (right panel) shows mean fluorescence intensity vs. time for differing TNF-α concentrations, mean ± SEM, with n = 2 channels for control and n = 3 channels for each concentration. (B) Three color experiment, in which fibrin (red), leukocytes (blue), and platelets (green) were tracked with distinct fluorophores. Left panel shows representative images of endothelialized channels pre-activated with varying doses (1 ng/mL vs. 10 ng/mL) of TNF- α. Quantitation (right panel) shows that platelets and fibrin vary with TNF-α concentration, but the number of adherent leukocytes is unchanged across doses, ** = $p < 0.01$, * = $p < 0.05$, # = n.s. ($p = 0.54$). (C) Use of brightfield

signal intensity as a marker of partially disrupted or fully occluded flow, following infusion of whole blood into TNF-α stimulated endothelialized channels. Representative image (left panel) shows characteristic increase in signal in bottom channel, which had occluded at the time point shown. Graph shows mean signal intensity (MSI) vs. time for differing TNF-α concentrations, mean ± SEM, with n = 2 channels for control and n = 3 channels for each concentration.

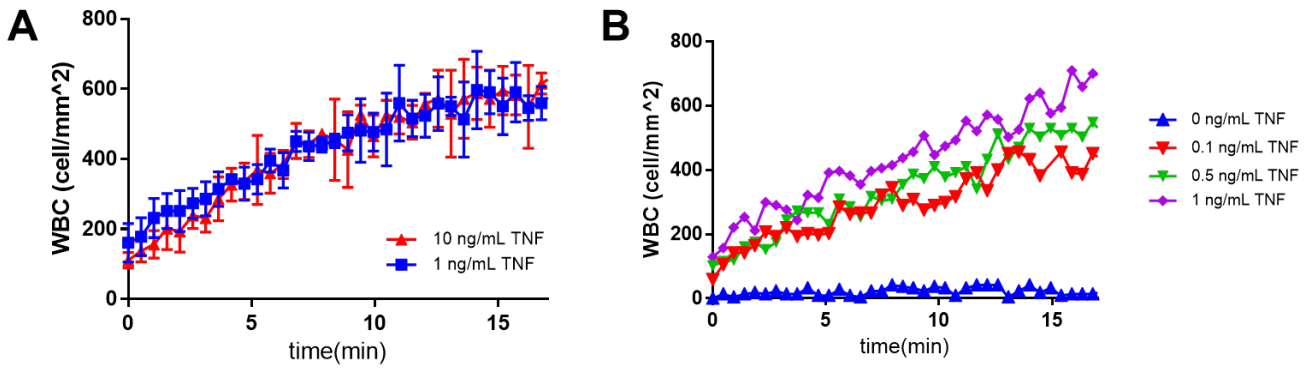

Figure S6. Quantification of leukocyte numbers in TNF-α activated channels. (A) Similar density of adhered leukocytes was observed between channels activated with either 1 ng/mL (blue) or 10 ng/mL (red)(n=3/dose) (B) A dose-response of adhered leukocytes was seen in a lower range of 0.1-1 ng/mL of TNF-α (n=1/dose). Minimal leukocyte adhesion was seen in un-activated channels (blue). The density of adhered leukocytes was calculated using an automated particle counting algorithm (ImageJ). Images from calcein-stained blood were converted to binary masks, and particles counted using the included “Analyze particles” algorithm with a circularity index of 0.5-1. To minimize interference from large platelet aggregates, blood was not recalcified prior to infusion over channels in these experiments.

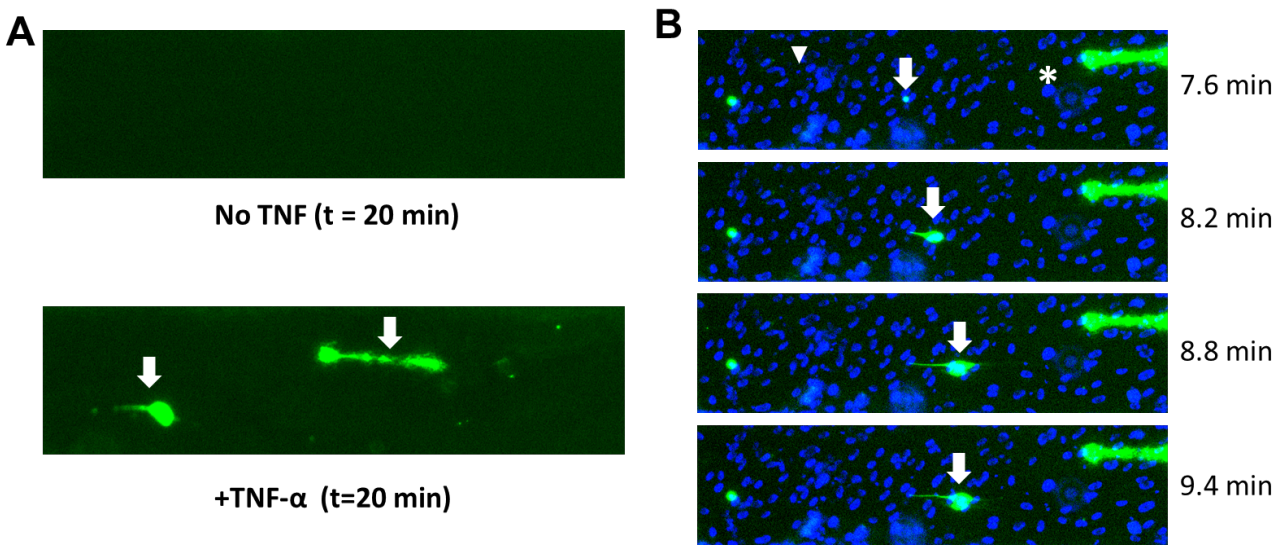

Figure S7. Exposure of TNF-α activated channels to whole blood results in deposition of neutrophil extracellular traps (NETs) enriched in nucleic acid. (A) Staining of extracellular nucleic acid, often in elongated deposits, was seen in TNF-alpha activated endothelium (bottom), but not in untreated channels (top). (B) Formation and growth of NETs could be monitored in whole blood in real time. Whole blood, stained with 1μM cell-impermeant SYTOX nucleic acid stain (green) and 4μM Hoeschst cell-permeant nucleic acid stain (blue), was infused over TNF-alpha (0.5 ng/mL) activated endothelium. Neutrophil nuclei could be seen as small, mobile, poly-lobated forms (arrowhead), while endothelial nuclei were larger, round, and stationary (asterisk). Extracellular DNA associated with NETs stained brightly with SYTOX, and dimly with Hoeschst (arrows).

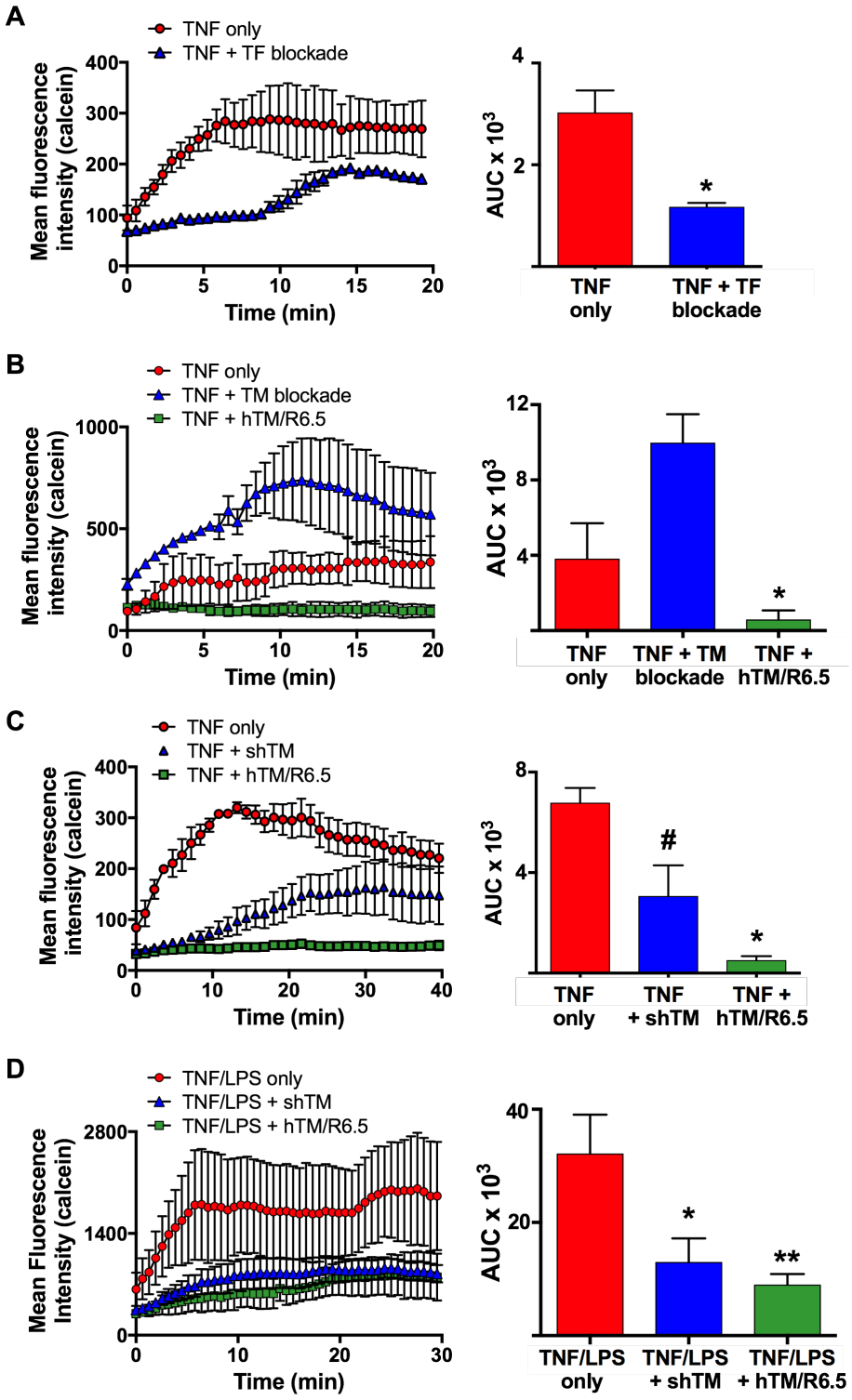

Figure S8. Green fluorescence time curves (left panel) and AUC analysis (right panel), mean ± SEM, from (A) TF inhibition experiment (n = 2 channels per condition, * - $p < 0.05$ vs. TNF only), (B) anti-TM vs. hTM/R6.5 experiment (n = 2 channels per condition, * - $p = 0.03$ for hTM/R6.5 vs. anti-TM), (C) shTM vs. hTM/R6.5 experiment (n = 2 channels per condition, * - $p = 0.03$ for hTM/R6.5 vs. TNF only, # - $p = 0.08$ for shTM vs.

TNF only), and (D) combined TNF/LPS model (n = 2 channels for TNF/LPS only and n = 3 channels for each treatment group, * - p = 0.04 for shTM vs. TNF/LPS only, ** - p = 0.02 for hTM/R6.5 vs. TNF/LPS only). The effect of each antibody and/or therapeutic on the accumulation of green fluorescence mirrored its effect on fibrin deposition (Figures 3A, 3B, 5B, and 6, respectively).

Condition	Time to peak (min, 95%CI)	Peak fibrin generation rate (MFI/min, 95% CI)
No TNF	N.D.	N.D.
1 ng/mL	17 (15,20)	5.4 (4.3,6.6)
10 ng/mL	4.4 (3.9,4.7)	13 (9,14)

Table S1 – Fibrin generation parameters as a function of TNF-alpha dose (values derived from the Gaussian fit of the average derivative curve, N.D. = no detectable fibrin generation)

Condition	Time to peak (min, 95%CI)	Peak fibrin generation rate (MFI/min, 95% CI)
No TNF	N.D.	N.D.
4 hr, 1 ng/mL TNF	22 (20,24)	10 (9.0,12)
6 hr, 1 ng/mL TNF	13 (13,14)	25 (23,27)

Table S2 – Fibrin generation parameters as a function of TNF-alpha time of expsoure (values derived from the Gaussian fit of the average derivative curve, N.D. = no detectable fibrin generation)

Condition	Time to peak (min, 95%CI)	Peak fibrin generation rate (MFI/min, 95% CI)
TNF	0.0 (0.0,0.0)	62 (53, 90)
TNF + anti-TF mAb	13 (13,13)	34 (32,36)

Table S3 – Fibrin generation parameters in response to anti-TF antibody(values derived from the Gaussian fit of the average derivative curve)

Condition	Time to peak (min, 95%CI)	Peak fibrin generation rate (MFI/min, 95% CI)
TNF	3.5 (0.0,5.1)	29 (21,37)
TNF + TM block	4.3 (3.6,4.8)	88 (80,95)
TNF + hTM/R6.5	N.D.	N.D.

Table S4 – Fibrin generation parameters in response to TM blockade or replishment with hTM/R6.5 (values derived from the Gaussian fit of the average derivative curve)

Condition	Time to peak (min, 95%CI)	Peak fibrin generation rate (MFI/min, 95% CI)
TNF	2.3 (2.0,2.7)	72 (68,77)
TNF + R6.5	2.6 (1.6,3.2)	52 (49,56)
TNF + shTM	3.6 (0.0,5.0)	49 (42,57)
TNF + hTM/R6.5	15 (13,17)	35 (32,41)

Table S5 – Fibrin generation parameters in response treatment with the indicated proteins during TNF-alpha washout period (values derived from the Gaussian fit of the average derivative curve)

Condition	Time to peak (min, 95%CI)	Peak fibrin generation rate (MFI/min, 95% CI)
TNF	12 (9.1,14)	4.7 (4.0,5.4)
TNF + shTM	33 (32,34)	1.6 (1.5,1.6)
TNF + hTM/R6.5	N.D.	N.D.

Table S6 – Fibrin generation parameters in response to treatment with shTM or hTM/R6.5(values derived from the Gaussian fit of the average derivative curve, N.D. = no detectable fibrin generation)

Condition	Time to peak (min, 95%CI)	Peak fibrin generation rate (MFI/min, 95% CI)
TNF	2.5 (4.3,5.1)	4.7 (4.3,5.1)
TNF + hirudin	11 (11,11)	3.4 (3.2,3.7)
TNF + hTM/R6.5	17 (16,19)	0.3 (0.2,0.3)

Table S7 – Fibrin generation parameters in response to treatment with hirudin or hTM/R6.5(values derived from the Gaussian fit of the average derivative curve)

Condition	Time to peak (min, 95%CI)	Peak fibrin generation rate (MFI/min, 95% CI)
TNF/LPS	4.8 (4.4,5.2)	110 (98, 130)
TNF/LPS + shTM	12 (8.9,14)	11 (8.9,14)
TNF/LPS + hTM/R6.5	21 (21,21)	5.7 (5.3,6.1)

Table S8 – Fibrin generation parameters in response TNF-alpha/LPS stimulation and treatment with either shTM or hTM/R6.5 (derived from the Gaussian fit of the average derivative curve)

Condition	Time to peak (min, 95%CI)	Peak fibrin generation rate (MFI/min, 95% CI)
TNF + control mAb	1.4 (1.0,1.8)	86 (82,91)
TNF + hTM/R6.5 + control mAb	17 (16,20)	17 (15,19)
TNF + APC1573	0.3 (0.0,1.0)	65 (59,74)
TNF + hTM/R6.5 + APC1573	3.8 (3.6,4.0)	70 (64,77)

Table S9 – Fibrin generation parameters in response to treatment hTM/R6.5 in the presence either APC-inhibitory or control antibodies (values derived from the Gaussian fit of the average derivative curve)

Condition	Time to peak (min, 95%CI)	Peak fibrin generation rate (MFI/min, 95% CI)
TNF, normal	**3.2 (2.9,3.4)**	**15 (14,17)**
TNF, PC deficient	**1.1 (0,1.7)**	**13 (12,15)**
TNF, normal + hTM/R6.5	**18 (16,30)**	**4.4 (3.6,7.1)**
TNF, PC deficient + hTM/R6.5	**8.0 (7.9,8.1)**	**15 (14,15)**

Table S10 – Fibrin generation parameters in response to treatment hTM/R6.5 in the either normal or PC-deficient plasma (values derived from the Gaussian fit of the average derivative curve)

Movies S1-S15

Movie S1. 3-D reconstruction of endothelialized channel. Endothelial cell nuclei are seen equally distributed along all 4 walls of microfluidic flow chamber.

Movie S2. Fluorescence microscopy of inflammatory thrombosis model. In the absence of TNF-α activation (bottom panel), neither fibrin deposition (red) nor leukocyte nor platelet adhesion (green) is seen over ~20 minutes of blood flow. In contrast, rapid accumulation of fluorescent signal is seen the top channel, treated with 10 ng/mL of TNF-α for 6 hours prior to infusion of WB.

Movie S3. Brightfield microscopy of inflammatory thrombosis model. Brightfield microscopy of the same channels shown in Movie S2. The top channel demonstrates the characteristic increase in signal intensity which accompanies disruption and eventual occlusion of blood flow.

Movie S4. Fibrin deposition varies with dose of TNF-α activation. Fluorescence microscopy shows earlier fibrin deposition in the bottom channel (10 ng/mL of TNF-α) than the top channel (1 ng/mL of TNF-α).

Movie S5. Fibrin deposition varies with duration of TNF-α activation. Fibrin deposition occurs earlier and to greater extent in the bottom channel, treated for 6 hours with 1 ng/mL of TNF-α, than the top channel, treated for 4 hours at the same dose.

Movie S6. Cellular adhesion varies with dose of TNF-α activation. Green fluorescence intensity, reflecting both leukocyte and platelet adhesion, accumulates earlier in the bottom channel, treated with 10 ng/mL of TNF-α x 6 hours, than in the top channel, treated with 1 ng/mL for the same time period.

Movie S7. Platelet adhesion and fibrin deposition, but not leukocyte adhesion, vary with TNF-α concentration. Fibrin (red), platelets (green), and leukocytes (blue) tracked with distinct fluorescent probes. Fibrin deposition and platelet adhesion are increased in the bottom channel (10 ng/mL of TNF-α x 6 hours) compared to the top channel (1 ng/mL x 6 hours).

Movie S8. Occlusion of blood flow at varying concentration of TNF-α activation. Brightfield microscopy shows disruption and occlusion of blood flow occurs earlier in the bottom channel, treated for 6 hours with 10ng/mL of TNF-α, than the top channel, treated for 6 hours with 1 ng/mL of TNF-α.

Movie S9. Blockade of endothelial tissue factor delays fibrin deposition. Antibody blockade of endothelial TF prior to the infusion of whole blood (top channel) delayed – but did not completely eliminate – coagulation in channels stimulated with 1 ng/mL of TNF x 6 hours. Bottom channel shows control without TF blockade.

Movie S10. Endothelial TM plays a critical role in regulating coagulation in DIC model. Contrasting effect of endothelial TM blockade (bottom channel) vs. replacement via hTM/R6.5 fusion protein (top channel). The former significantly increases, whereas the latter completely eliminates, fibrin deposition in this model.

Movie S11. Comparison of antithrombotic effect of shTM vs. hTM/R6.5. Although both antithrombotic agents significantly delay and decrease fibrin deposition (video represents > 40 minutes of blood flow), shTM mixed in the whole blood at a concentration of 100 nM (top channel) is less effective than hTM/R6.5 anchored to the endothelial luminal membrane (bottom channel).

Movie S12. Comparison of antithrombotic effect of hirudin vs. hTM/R6.5. Similar results are seen when recombinant hirudin, a direct thrombin inhibitor, added to whole blood at a concentration of 5 U/mL (top channel), is compared to the bottom channel, treated with hTM/R6.5 (50 nM) prior to infusion of whole blood.

Movie S13. hTM/R6.5 and shTM in combined model. hTM/R6.5 (top channel) demonstrates superior antithrombotic effect compared to shTM (bottom channel) following combination of TNF-α (1 ng/mL x 6 hours) and LPS activation of WB (50 ng/mL x 90 min).

Movie S14. Antithrombotic activity of hTM/R6.5 is dependent on PC activation. Addition of hAPC inhibitory antibody to WB (bottom channel), as compared to isotype control antibody (top channel), inhibits the antithrombotic effect of hTM/R6.5.

Movie S15. Exogenous PC restores anti-thrombotic activity of hTM/R6.5 in PC deficient blood. Antithrombotic effect of hTM/R6.5 is diminished in PC deficient blood (top channel) and restored by addition of plasma-derived human PC concentrate (bottom channel).